Convergent extension movements in growth plate chondrocytes require gpi-anchored cell surface proteins

Molly J. Ahrens[1], Yuwei Li[1], Hongmei Jiang[2] and Andrew T. Dudley[1],*

Proteins that are localized to the cell surface via glycosylphosphatidylinositol (gpi) anchors have been proposed to regulate cell signaling and cell adhesion events involved in tissue patterning. Conditional deletion of *Piga*, which encodes the catalytic subunit of an essential enzyme in the gpi-biosynthetic pathway, in the lateral plate mesoderm results in normally patterned limbs that display chondrodysplasia. Analysis of mutant and mosaic *Piga* cartilage revealed two independent cell autonomous defects. First, loss of *Piga* function interferes with signal reception by chondrocytes as evidenced by delayed maturation. Second, the proliferative chondrocytes, although present, fail to flatten and arrange into columns. We present evidence that the abnormal organization of mutant proliferative chondrocytes results from errors in cell intercalation. Collectively, our data suggest that the distinct morphological features of the proliferative chondrocytes result from a convergent extension-like process that is regulated independently of chondrocyte maturation.

KEY WORDS: Glycosylphosphatidylinositol (gpi), Chondrocyte, Polarity, Morphogenesis, Convergent extension

INTRODUCTION

Growth of endochondral bones derives from regulation of the rate of chondrocyte maturation in the growth plate cartilage (reviewed by Kronenberg, 2003). In the growth plate, resting chondrocytes are a pool of progenitor cells that reside at the ends of embryonic long bones (Abad et al., 2002). Resting chondrocytes mature into proliferative chondrocytes that are characterized by the upregulation of cell proliferation and a change in cell morphology, such that round resting cells give rise to proliferative progeny that are discoid and arranged in columns resembling a stack of coins (Dodds, 1930). As maturation continues, proliferative chondrocytes undergo cell cycle arrest and enlarge, forming prehypertrophic cells. Subsequently, these cells undergo extensive growth to form hypertrophic chondrocytes, which deposit a specialized cartilage matrix that serves as a scaffold for blood vessels and osteoblasts to invade and lay down a true bony matrix (Howlett, 1979; Howlett, 1980; Noonan et al., 1998; Hunziker et al., 1999).

Establishment and maintenance of this cellular architecture is essential for proper function of the growth plate. Previous studies have revealed a complex network of interacting signaling pathways that generate a robust system to regulate the growth plate cartilage. At the heart of this system lie the secreted signaling proteins Indian hedgehog (Ihh) and parathyroid hormone-related peptide (Pthrp; also known as Pthlh) (reviewed by Kronenberg, 2003). Ihh produced by the prehypertrophic chondrocytes acts to induce proliferative chondrocyte formation while simultaneously inducing Pthrp expression in resting chondrocytes (Vortkamp et al., 1996). In turn, Pthrp secreted by resting chondrocytes antagonizes both the action of Ihh and the maturation of proliferative chondrocytes into prehypertrophic chondrocytes. Overlaid on this central interaction are the antagonistic actions of the Wingless/Int-1 factors Wnt5a and Wnt5b that coordinately control the transitions from resting to proliferative and

proliferative to prehypertrophic chondrocyte (Yang et al., 2003). Bone morphogenetic proteins (Bmp) and fibroblast growth factors (Fgf) provide additional regulation of chondrocyte maturation (Kronenberg, 2003). Together, these positive and negative interactions help to establish distinct zones of resting, proliferative, and hypertrophic chondrocytes.

Previously, we demonstrated that columns of proliferative chondrocytes form by a process of convergent extension (CE) involving cell intercalation (Li and Dudley, 2009). Thus, cell division displaces daughter cells lateral to the column before cell intercalation movements promote re-integration. Orientation of the division plane and the stacking of chondrocytes depend on non-canonical frizzled (Fzd) signaling and Rho GTPase activity, two components of pathways that additionally regulate CE movements in the neural tube and planar cell polarity (PCP) in epithelial tissues (Klein and Mlodzik, 2005). Proteins displayed on the cell surface via glycosylphosphatidylinositol (gpi) linkages are also important components of the CE pathway (Topczewski et al., 2001; Shao et al., 2009), and reduction in gpi-anchored proteins affects CE in the axolotl and zebrafish (Drawbridge and Steinberg, 2000; Shao et al., 2009). Therefore, we sought to determine whether gpi-anchored proteins are also key regulators of CE and PCP in other tissues.

Gpi-anchored proteins include heparan sulfate proteoglycans (HSPGs) of the glypican family, ephrin A ligands (for Eph receptors), putative adhesion/signaling molecules of the Ly6 family, and enzymes such as alkaline phosphatase (Bernfield et al., 1999; Paulick and Bertozzi, 2008). In addition to regulating CE movement, gpi-anchored proteins are thought to play important roles in patterning tissue by regulating cell signaling and cell adhesion. For example, loss of the glypican Dally interferes with Wingless (Wg) signaling and results in defects in patterning of the ventral denticles and wing of *Drosophila* (Lin and Perrimon, 1999; Tsuda et al., 1999). In vertebrates, manipulation of gpi-anchored ephrin A (Ide et al., 1994; Wada and Ide, 1994; Stadler et al., 2001), a ligand for Eph receptors, or of the ortholog of the gpi-anchored Ly6 family protein CD59 (da Silva et al., 2002; Kumar et al., 2007) in the limb mesenchyme results in defects in cell sorting and skeletal patterning. Therefore, gpi-anchored proteins might mediate the cellular interactions that impart unique identities to subgroups of cells within a field to promote tissue patterning.

[1]Department of Biochemistry, Molecular Biology and Cell Biology, Northwestern University, 2205 Tech Drive, Evanston, IL 60208, USA. [2]Department of Statistics, Northwestern University, 2006 Sheridan Road, Evanston, IL 60208, USA.

*Author for correspondence (a-dudley@northwestern.edu)

Simple genetic tests of these models are confounded by the presence of diverse families of gpi-anchored molecules. As a first approach, we knocked out display of all gpi-anchored proteins on the cell surface using a conditional allele of *Piga*, which encodes the catalytic subunit of the enzyme complex that generates gpi moieties (Kawagoe et al., 1994; Keller et al., 1999; Keller et al., 2001). Conditional deletion of *Piga* in the lateral plate mesoderm (LPM) – progenitors of the limb skeleton – surprisingly resulted in a normally patterned limb skeleton. Here, we show that *Piga* null chondrocytes have normal maturation signatures, but abrogation of gpi-anchors causes cell autonomous defects in maturation rate, in cell morphology, and in chondrocyte organization. Although chondrocytes progress through each stage of the maturation process, mutant growth plates fail to form columns of discoid chondrocytes. Failure of column formation results from a defect in cell intercalation, a coordinated cell movement that depends on cell polarity. In addition, *Piga* expression is required to properly orient hair cells in the inner ear, a process regulated by the PCP pathway. Collectively, our data firmly establish that gpi-anchored proteins are common components of polarity pathways, including one that regulates CE-like movements in proliferative chondrocytes that in part define the structure and the growth properties of developing long bones.

MATERIALS AND METHODS

Mouse strains and animal care
The mouse strains used are *Hoxb6::cre* (Lowe et al., 2000), *lox-Piga-lacZ* (Tremml et al., 1999), *Prx1-cre* (Logan et al., 2002), *Ctnnb1*[tm2Kem] (Brault et al., 2001), *Foxg1*[tm1(cre)Skm] (Hebert and McConnell, 2000), and *TOPGAL* [Jackson Laboratories (DasGupta and Fuchs, 1999)]. Animal care and use was in accordance with NIH guidelines and was approved by the Animal Care and Use Committee of Northwestern University. The morning after mating was designated as 0.5 days post coitum (dpc).

Histology
Skeletons were prepared as described (McLeod, 1980). Briefly, dissected hindlimbs were dehydrated in 95% ethanol followed by acetone, stained with Alcian Blue/Alizarin Red (Sigma), washed in 95% ethanol, cleared with 1% KOH, followed by a glycerol/decreasing KOH series, and stored in 100% glycerol.

To analyze cell morphology, limbs were dissected, fixed in Bouin's Fixative (Ricca Chemical Company, Texas, USA) at 4°C overnight, dehydrated through an ethanol series followed by xylenes, and embedded in paraffin (Richard-Allan Scientific, MI, USA). Sections were stained with Masson's Trichrome using a standard protocol.

β-galactosidase staining on P0 hindlimbs from TOPGAL mice was performed as described (Kawaguchi et al., 2002). Briefly, limbs were fixed in 1% paraformaldehyde (PFA)/0.5% glutaraldehyde in PBS for 1.5 hours at room temperature, and then stained in X-gal staining solution at 37°C overnight.

Antibody staining
To analyze cell proliferation, cells in S-phase were labeled with bromodeoxyuridine (BrdU) for 2 hours prior to tissue harvest. Tissue was fixed in 4% PFA in PBS at 4°C overnight and prepared for paraffin sectioning as described. Sections of BrdU-labeled tissue were digested in trypsin and depurinated in hydrochloric acid. Incorporated BrdU was detected using a mouse anti-BrdU monoclonal antibody (Developmental Studies Hybridoma Bank, Iowa, USA) and Cy2-labeled donkey anti-mouse antibody (Jackson ImmunoResearch Laboratories, Pennsylvania, USA). Nuclei were counterstained with 4′,6-diamidino-2-pheylindole (DAPI, Sigma-Aldrich). The BrdU labeling index was calculated as the percentage of total nuclei that were BrdU positive in each designated box.

P0 cryosections were used for staining with the following antibodies: cleaved caspase-3 (1:500, Cell Signaling); phospho-Smad 1(Ser463/465), 5(Ser 463/465) and 8(Ser 426/428; 1:500, Cell Signaling); phospho-p44/42 (1:100, Cell Signaling); β-galactosidase (1:2000, a gift from R. Holmgren,

Northwestern University, IL, USA); acetylated tubulin (1:1000, Sigma). Samples were washed in PBS plus 0.1% Triton X-100 (PBSTx), blocked for 1 hour in 10% FBS/PBSTx at room temperature, then incubated overnight at 4°C with the primary antibody in 2% FBS/PBSTx. Samples were washed and incubated with donkey anti-rabbit Alexa 488 (1:500, Invitrogen) for 4 hours at room temperature, and counterstained with DAPI.

Gene expression analysis
For in situ hybridization (ISH) analysis, RNA probes were produced using T7, T3 or SP6 polymerase in the presence of non-radioactive digoxigenin-labeled rNTPs (Roche) or S[35] (PerkinElmer), as described (Murtaugh et al., 1999). For quantification, the length of the expression domain was measured along the longitudinal axis of the cartilage and calculated as a ratio over the total length of the growth plate (articular surface to the mineralized region) using non-radioactive samples.

Chondrocyte isolation and culture
Growth plate cartilage was dissected free of the perichondrium/periosteum, minced with a razor blade, and incubated in 0.5% collagenase in DMEM+10% heat inactivated FBS (Invitrogen) at 37°C for 3 hours. After gentle trituration the resulting cell suspension was passed through a cell strainer (70 μm pore size, Becton-Dickinson), pelleted, and washed twice with serum-free DMEM. For transfection experiments, 2.5×10^5 chondrocytes were seeded into 12-well tissue culture clusters (Corning) in DMEM+10% heat-inactivated serum with penicillin/streptomycin. Eighteen to 24 hours later chondrocytes were transfected with GFP-gpi or GFP-myr (gifts from A.-K. Hadjantonakis, Sloan-Kettering Institute, NY, USA) using Superfect transfection reagent (Qiagen), according to the manufacturer's instructions. Thirty-six hours later, cultures were washed twice with PBS and imaged by epifluorescence.

Flow cytometry
All incubations were performed on ice in PBS containing 0.1% sodium azide unless otherwise noted. Isolated chondrocytes were washed three times in PBS/azide, blocked in 5% heat-inactivated normal donkey serum (Jackson ImmunoResearch), and incubated for 4 hours in 5% serum containing 1 μg/10^5 chondrocytes of sheep IgG (Jackson ImmunoResearch) or anti-Gpc3 (R&D Systems). After washing three times in PBS/azide, cells were incubated in Alexa-Fluor 488-anti-sheep antibody (Invitrogen) for 1 hour. Cells were washed three times in PBS/azide then fixed in 2% PFA and analyzed using a FACScalibur and Cell Quant Pro software (Becton-Dickinson). For experiments involving removal of gpi-anchored proteins, cells were initially incubated in αMEM (Invitrogen) containing 0.1 units of gpi-specific phospholipase C (Sigma Aldrich) for 1 hour at 37°C.

Alkaline phosphatase activity
P3 limbs were fixed in 4% PFA for 3 hours at room temperature and then prepared for cryosectioning. Alkaline phosphatase staining was performed as described in the development step of the non-radioactive ISH protocol.

Image analysis
Orientation of cell division was determined as described (Li and Dudley, 2009). For analysis of stereocilia, P0 *lox-Piga-lacZ/Foxg1*[tm1(cre)Skm] pup inner ears were dissected in PBS/2 mM CaCl$_2$/0.5 mM MgCl$_2$ and fixed in 4% PFA/2 mM CaCl$_2$/0.5 mM MgCl$_2$ at 4°C overnight. The following day, the cochlea were dissected from the temporal bone, and the tissue was permeabalized in PBS plus 1% Triton X-100 (PBSTx) for 1-2 hours, and then blocked overnight in 20% heat-inactivated sheep serum/PBSTx. Cochlea were stained with anti-acetylated tubulin (1:200, Sigma) to visualize the kinocilium or anti-Vangl2 (1:400, gift from M. Montcouquiol, INSERM, Bordeaux, France). All specimens were additionally incubated with Alexa-Fluor 568 phalloidin (Invitrogen) to label the stereocilia and actin cytoskeleton. Images were acquired using a Zeiss apotome deconvolution microscope or Leica Confocal Laser Scanning System and analyzed as described (Qian et al., 2007).

Statistical methods
A two-way ANOVA was used to determine whether the distributions of gene expression domain length were distinct between wild-type and mutant mice. The model contained the main effects of genotype (wild type and mutant) and
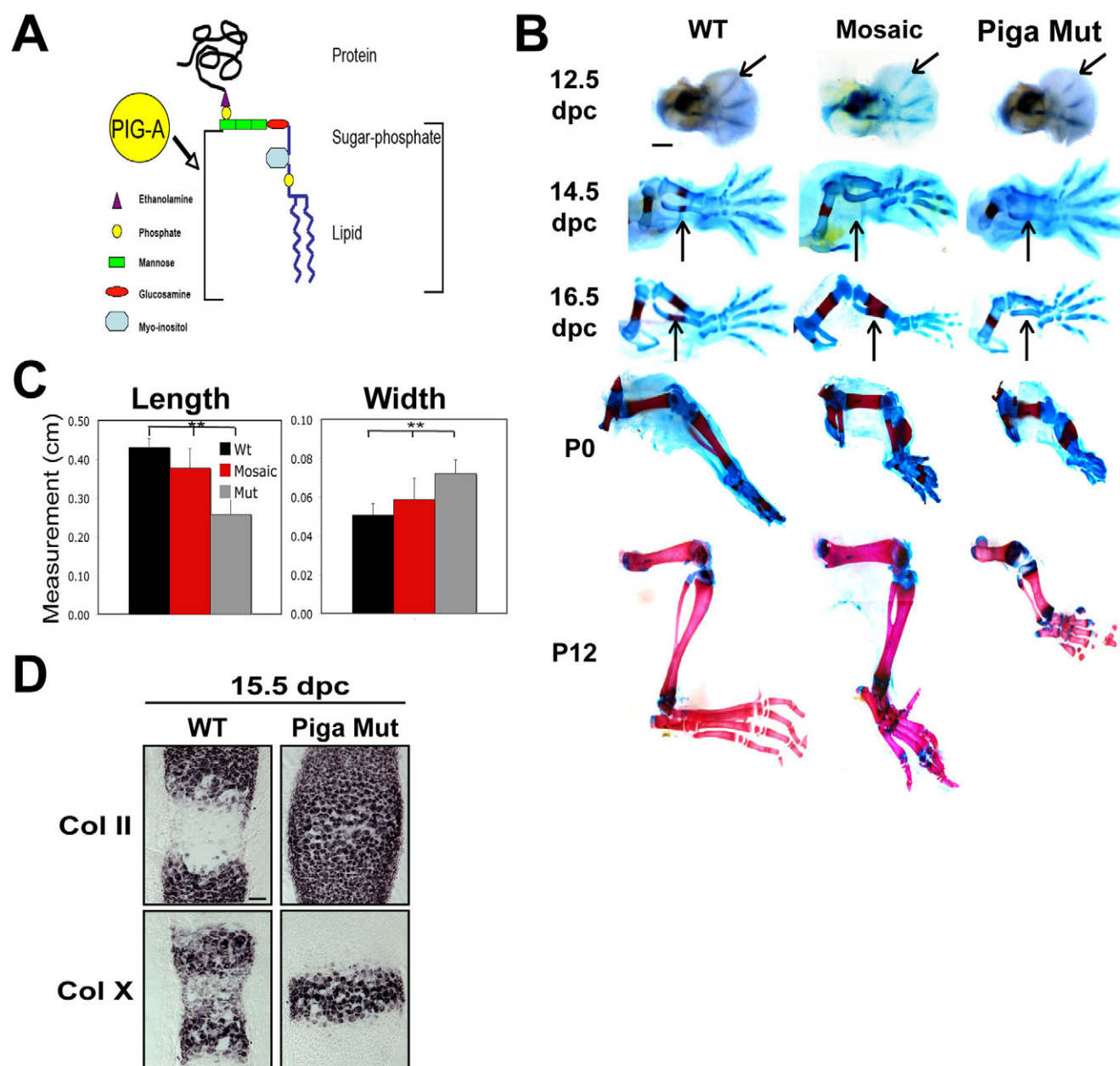
Fig. 1. Chondrodysplasia in *Piga* mutant limbs. (**A**) Gpi-anchored proteins are composed of a lipid tail, a sugar-phosphate linkage, and a protein. (**B**) Alcian Blue and Alizarin Red staining show a delay in cartilage formation beginning at 12.5 dpc (black arrow) and a delay in mineralization at 14.5 dpc and 16.5 dpc in mutant samples (black arrow). At P0 and P12, mutant bones are mineralized but shorter than wild type. (**C**) At P0, mutant bones are significantly shorter (*P*<0.0001) and wider (*P*<0.0001) than wild type. Heterozygous females (mosaic) have an intermediate length (wild type versus mosaic, *P*=0.0004; mutant versus mosaic, *P*<0.0001) and width (wild type versus mosaic, *P*=0.003; mutant versus mosaic, *P*=0.0001). (**D**) *Col2a1* expression in immature cartilage is found in both wild-type and mutant limbs. Hypertrophic chondrocytes expressing *Col10a1* persist in the diaphysis of mutant bones at 15.5 dpc. Scale bars: in B, 50 μm for 12.5 dpc and 14.5 dpc, 100 μm for 16.5 dpc and P0, 125 μm for P12; in D, 100 μm.

zone (an interaction effect between the genotype and zone). Different contrasts were constructed to test whether the gene expression of a particular zone was the same between wild-type and mutant mice; if two zones had the same gene expression within the same genotype; and if the gene expression difference between two zones of interest was the same for wild type and mutants. Bonferroni's procedure was used to control the family-wise error rate at significance level 0.05 as multiple tests were performed simultaneously. That is, a test was considered to be statistically significant if the corresponding *P*-values were below 0.05 divided by the total number of tests. Analysis was based on a minimum of three independent samples per genotype.

RESULTS
Chondrodysplasia in *Piga* mutant limbs
To determine the role of gpi-anchored proteins in development, we analyzed loss of *Piga* expression in developing limbs. *Piga* encodes PIG-A, the catalytic subunit of an essential enzyme for the initial step of gpi-anchor biosynthesis (Fig. 1A) (Miyata et al., 1993; Watanabe et al., 1998; Kostova et al., 2000). Since null *Piga* alleles are early embryonic lethal (Kawagoe et al., 1994; Rosti et al., 1997), a conditional allele was employed to selectively delete *Piga* using
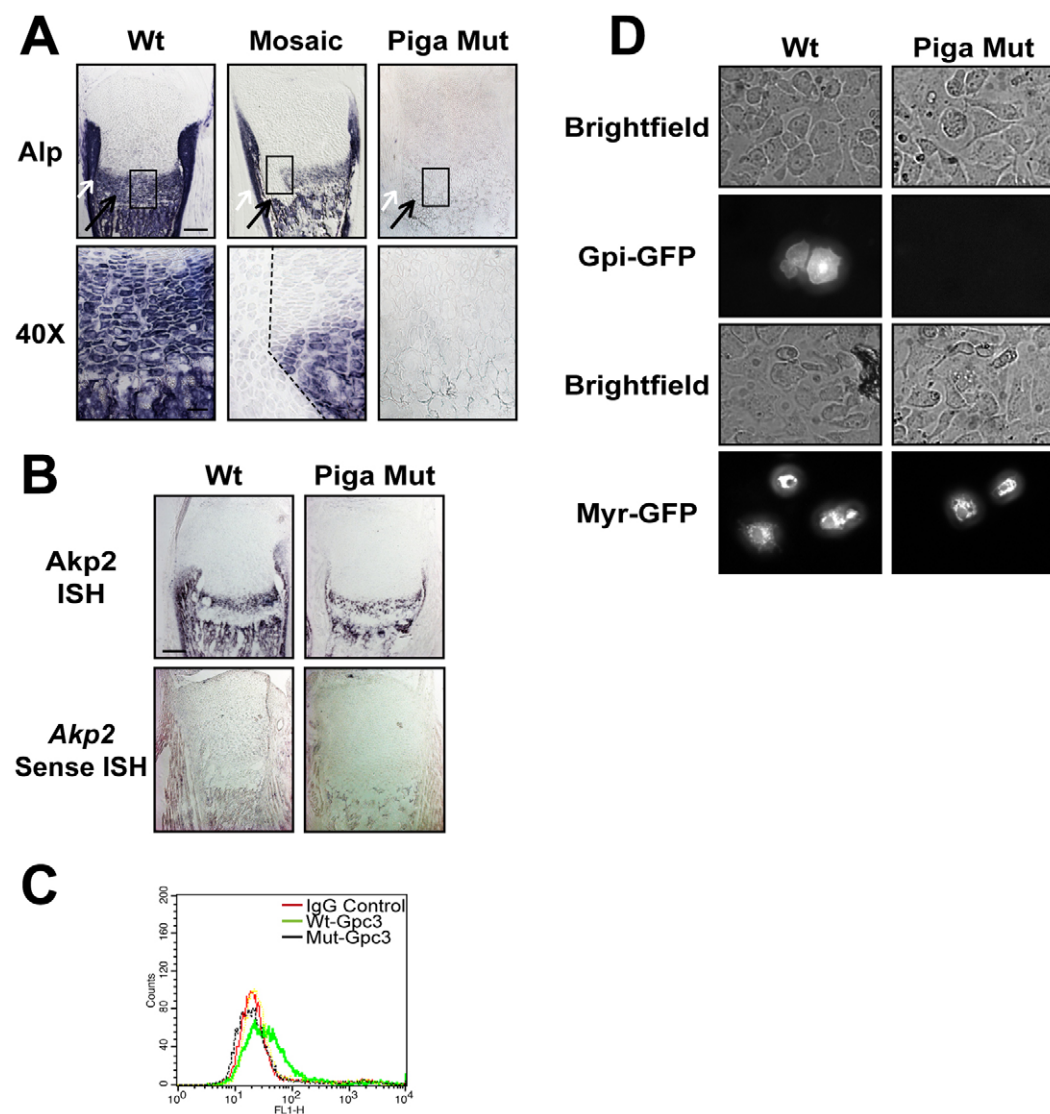
**Fig. 2.** *Piga* mutant cartilage lacks gpi-anchored proteins. (**A**) Alkaline phosphatase (Alp) activity is analyzed in wild-type (Wt), mosaic, and mutant (Mut) growth plates. The black arrows highlight the chondrocytes and the white arrows point to the perichondrium. The black dashed line in the mosaic sample demarcates the boundary between mutant (left) and wild-type (right) chondrocytes. Alp-positive cells only derive from columnar proliferative chondrocytes. (**B**) ISH for *Akp2* reveals normal expression profiles in wild-type and *Piga* mutant growth plates. No signal is observed with the sense probe. (**C**) Flow cytometry shows that *Piga* mutant (black) chondrocytes lack Gpc3 and have comparable fluorescence to IgG controls (red), in contrast to wild-type chondrocytes that have increased fluorescence (green). (**D**) Transfected wild-type chondrocytes display gpi-Gfp on the cell surface but *Piga* mutant chondrocytes do not. Localization of myristolated-Gfp is similar in wild-type and mutant transfected cells. Scale bars: in A, 200 µm for 10× images, 50 µm for 40× images; in B, 200 µm.

Cre recombinase (Keller et al., 1999; Tremml et al., 1999). We took advantage of the fact that *Piga* resides on the X chromosome and mated females homozygous for the conditional allele (X^{Piga}/X^{Piga}) to males heterozygous for the autosomal *Hoxb6::cre* transgene (*cre/+*) that expresses Cre recombinase in the posterior LPM (Lowe et al., 2000), which gives rise to the mesenchyme from which the hindlimb skeleton forms. Analysis using reporter alleles shows that *Hoxb6::cre* transgene function is initiated at 8.5 days post coitum (dpc) and promotes near complete recombination in the hindlimb mesenchyme by 9.5 dpc prior to limb bud outgrowth (Lowe et al., 2000). Our breeding scheme yields equal numbers of genotypically wild-type ($X^{Piga}Y$; +/+) and mutant ($X^{Piga}Y$; *cre/+*) males (data not shown). By contrast, all females are heterozygous for the conditional allele (X^{Piga}/X). However, due to random X-inactivation, females carrying the *Hoxb6::cre* transgene (X^{Piga}/X; *cre/+*) are mosaics composed of both wild-type and null cells. The following studies are based on the analysis of both null mutant ($X^{Piga}Y$; *cre/+*) and mosaic (X^{Piga}/X; *cre/+*) limbs.

Given the proposed roles for gpi-anchored proteins in embryogenesis, we were surprised to find normal patterning of the limb skeleton in both mutant and mosaic animals (Fig. 1B). The slight delay in formation of distal cartilage elements that was observed at 12.5 dpc did not translate into patterning defects at later stages. However, *Piga* mutant hindlimb long bones were significantly shorter (*P<0.0001*) and wider (*P<0.0001*) at birth, although heterozygous females presented an intermediate phenotype (Fig. 1C).

A substantial delay in ossification was observed at 14.5 dpc but was absent twelve days after birth (P12). By 15.5 dpc, wild-type cartilage displayed domains of collagen type X alpha 1 (*Col10a1*)-positive hypertrophic chondrocytes between the collagen type II alpha 1 (*Col2a1*)-expressing immature chondrocytes and the primary ossification center (Fig. 1D). By contrast, only a single small domain of *Col10a1* expression occupies the central diaphysis in *Piga* mutants. Furthermore, a reduction in mineralization was observed in the periosteum and the primary ossification center at birth, and *Piga* mutants did not form an extensive trabecular network as observed in wild-type cartilage (see Fig. S1 in the supplementary material). Because matrix mineralization is one function of osteoblasts, we investigated whether gpi-anchored proteins are required for osteoblast formation. Analysis of collagen type I alpha 1 (*Col1a1*), osteocalcin (*OC*; also known as *Bglap2*) and osteopontin (*Opn*; also known as *Spp1*) suggested normal or slightly decreased numbers of mature and progenitor osteoblasts (Kratochwil et al.,
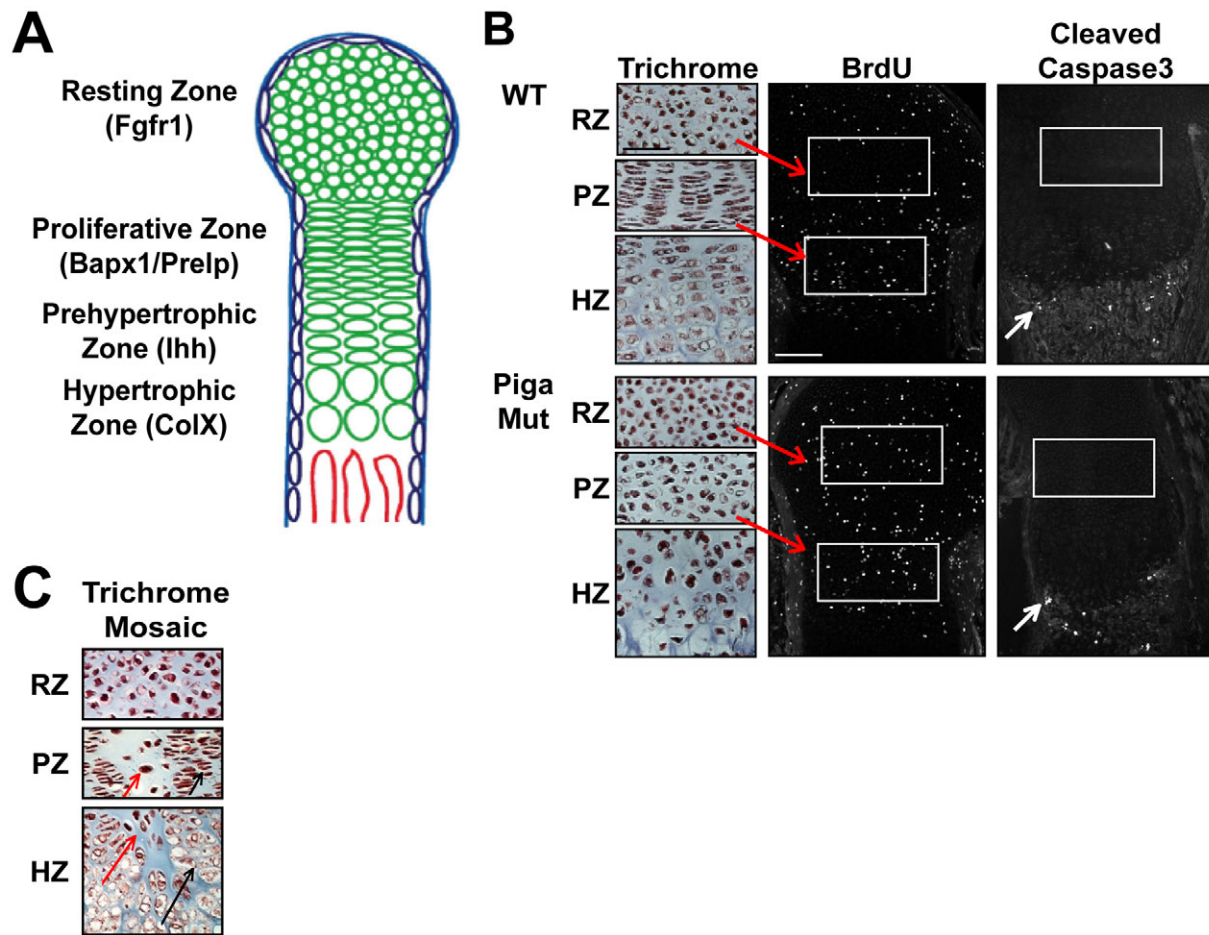
Fig. 3. Chondrocyte organization is altered in *Piga* mutant limbs. (**A**) The growth plate contains distinct zones, including resting (RZ), proliferative (PZ), prehypertrophic, and hypertrophic chondrocyte (HZ) zones. (**B**) Masson's trichrome-stained sections of P0 cartilage reveals that the transition from round disorganized cells to discoid columns is perturbed in *Piga* mutant chondrocytes. BrdU staining shows that the proliferation rate in *Piga* mutant RZ is increased compared with in wild type (9.8±0.2% versus 5.7±0.7%); the proliferation rate is increased in the RZ of *Piga* mutants compared with wild type (14.7±2.2% versus 12.3±1.6%). Cleaved caspase 3 antibody staining shows that apoptosis is absent in the growth plate (box) and normal in mineralized regions (arrow). (**C**) Trichrome staining of mosaic growth plates demonstrates that stacked discoid wild-type chondrocytes (black arrow) are found adjacent to round disorganized mutant chondrocytes (red arrow). Scale bars in B: 50 µm for trichrome staining; 100 µm for immunostaining.

1993; Sommer et al., 1996). Thus, gpi-anchored proteins are not required for skeletal patterning or osteoblast formation, but might have additional roles in osteoblast cells.

Gpi-anchored proteins are absent from *Piga* mutant chondrocytes

The absence of major developmental defects could result from a perdurance of gpi-anchored proteins produced prior to recombination or from partial compensation of *Piga* function by other cellular enzymes. To test these possibilities, we examined whether gpi-anchored proteins were lost in *Piga* mutant chondrocytes. Alkaline phosphatase (Alp) is a gpi-anchored enzyme displayed on the surface of hypertrophic chondrocytes and osteoblasts. Alp activity was not detectable in *Piga* null cartilage, but in situ hybridization (ISH) analysis confirmed expression of *Akp2* (also known as *Alpl*), the gene encoding bone/liver/kidney alkaline phosphatase (Fig. 2A,B) (Pizauro et al., 1994; Magnusson et al., 1999). Interestingly, in mosaic females, we observed clusters of Alp-positive cells generated from morphologically wild-type columnar chondrocytes beside Alp-negative cells generated from

round mutant chondrocytes (Fig. 2A). The phenotypes appeared to remain spatially segregated, as 'salt-and-pepper' patterns were never observed with regard to cell shape or Alp activity. We additionally showed by flow cytometry that the gpi-anchored protein glypican 3 (Gpc3) is not displayed on *Piga* mutant chondrocytes (Fig. 2C; see also Figs S2, S3 in the supplementary material). Moreover, mutant chondrocytes transfected with gpi-anchored green fluorescent protein (*gfp*) lacked fluorescence in contrast to wild-type chondrocytes (Fig. 2D). By contrast, transfection with a myristolated *gfp* construct resulted in equivalent fluorescence on intracellular membranes of wild-type and mutant chondrocytes (Fig. 2D). Together, these data demonstrate that gpi-anchored proteins are absent from the cell surface of *Piga* mutant chondrocytes.

Piga mutant chondrocytes proceed through normal stages of maturation

The observation of morphologically abnormal chondrocytes suggested the presence of defects in chondrocyte maturation in mutants. To determine whether loss of *Piga* expression affects early steps in chondrocyte maturation, we first examined the cellular

structure of developing tibiae. In *Piga* null hindlimbs, resting chondrocytes appeared normal but proliferative chondrocytes failed to flatten or form columns (Fig. 3A,B). Heterozygous females are mosaics with round mutant chondrocytes adjacent to discoid wild-type chondrocytes (Fig. 3C). Bromodeoxyuridine incorporation (Fig. 3B) demonstrated upregulation of the cell cycle in the growth plate cartilage of wild-type (5.7±0.7% versus 12.3±1.6%, resting versus proliferative chondrocytes) and mutant (9.8±0.2% versus 14.7±2.2%, resting versus proliferative chondrocytes) samples. Curiously, we observed a small but significant increase in cell proliferation in mutants compared with littermate controls (e.g. 9.8±0.2% versus 5.7±0.7%, in the resting chondrocytes). In addition, the absence of cleaved caspase-3-positive apoptotic chondrocytes demonstrates that cell viability does not depend on gpi-anchored proteins (Fig. 3B) (Nicholson et al., 1995). Upregulation of the cell cycle suggests that *Piga* growth plates contain proliferative chondrocytes. To test this possibility, we used ISH analysis to show that mutant growth plate chondrocytes expressed markers appropriate to immature (*Col9a1*) chondroctyes of the resting (*Fgfr1*) and proliferative (*Bapx1*, *Fgfr3*, *Prelp*) zones, prehypertrophic chondrocytes (*Ihh*), and hypertrophic chondrocytes (*Col10a1*; see Fig. S4 in the supplementary material; see also Fig. 4A). Thus, *Piga* null growth plates contain a bona fide proliferative zone.

Although each is present, the length of some maturation zones is altered in mutants indicating imbalances in chondrocyte maturation. To quantify this effect, we measured the length of gene expression domains along the epiphyseal-metaphyseal axis and determined the ratio of this measurement to total length of the growth plate (articular surface to the mineralized region). These measurements revealed that total growth plate length is similar at birth (P0) for wild-type (1.05±0.16 mm), mosaic (1.03±0.10 mm) and mutant (1.04±0.16 mm) femurs. The domain of least mature chondrocytes was not significantly shorter in mutants compared with wild type (Fig. 4B; *Fgfr1*, P=0.033) unlike, the proliferative (*Prelp*, P<0.0001) and prehypertrophic zones (*Ihh*; P<0.005; Fig. 4B). By contrast, the region between the *Fgfr1* and the *Prelp* expression domains was expanded (P<0.0001), consistent with the observed upregulation of cell proliferation (Fig. 4B). Collectively, our results demonstrate that morphologically abnormal *Piga* mutant chondrocytes undergo normal phases of maturation and that the delay in maturation begins at the transition between resting and proliferative chondrocytes.

Additionally, we compared the length of gene expression domains for wild-type and null cells in mosaic cartilage. The *Prelp* expression domain was similar in size for wild-type chondrocytes in both mosaic and wild-type growth plates (P=0.062; Fig. 5A,B). Similarly, the expression domain of *Ihh* was the same for wild-type cells in mosaic and wild-type samples (P=0.364; Fig. 5A,B). Likewise, gene expression domains were similar for mutant chondrocytes expressing *Prelp* (P=0.944) and *Ihh* (P=0.610; Fig. 5A,B), whether the *Piga* null cells were in a mutant or a wild-type environment. The delayed maturation of *Piga* mutant chondrocytes in mosaic cartilage suggests a defect in signal reception. However, we did not detect a decrease in Ihh, Bmp, Fgf, or canonical Wnt signaling in mutant chondrocytes (Fig. 4A,B, *Ptc1*; see Fig. S5 in the supplementary material; see also Fig. 6C). Moreover, to confirm that canonical Wnt signaling is unaffected, we demonstrated that conditional inactivation of β-catenin (*Ctnnb1^tm2Kem*) (Brault et al., 2001) in the cartilage does not alter morphology or organization of proliferative chondrocytes (Fig. S6 in the supplementary material).
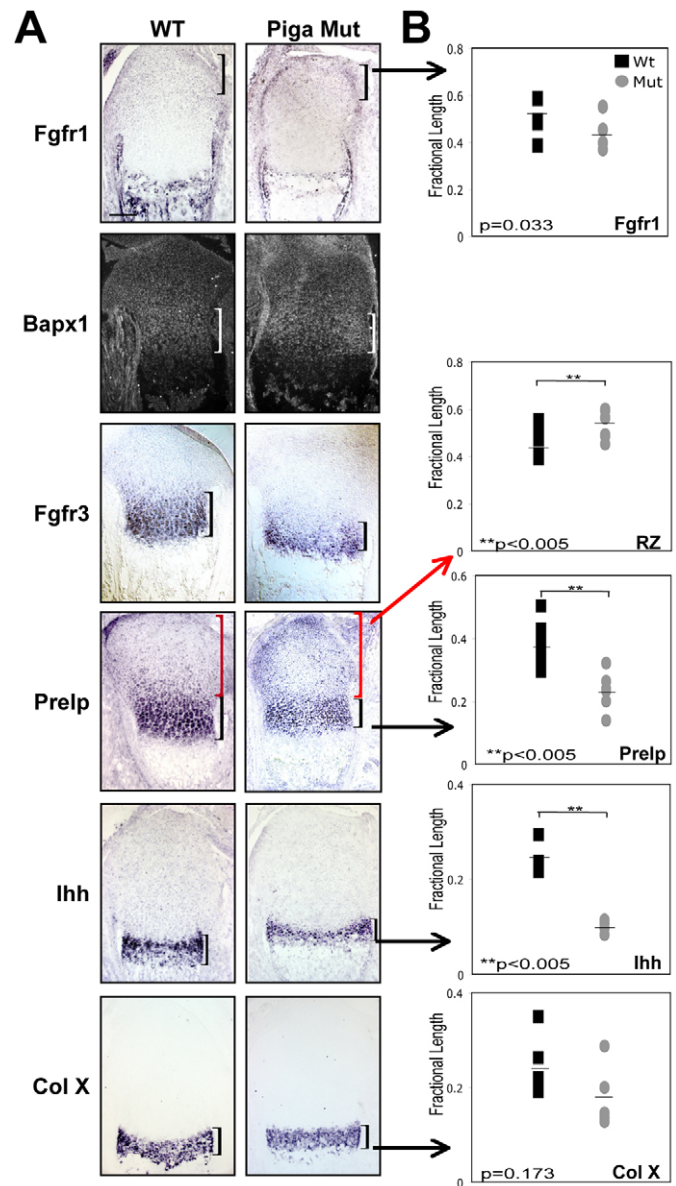
Fig. 4. *Piga* mutant chondrocytes undergo normal stages of maturation. (**A**) Each zone is present in *Piga* mutant growth plates as evidenced by ISH using the following markers: fibroblast growth factor receptor 1 (*Fgfr1*), bagpipe (*Bapx1*), fibroblast growth factor receptor 3 (*Fgfr3*), proline/arginine-rich end leucine-rich repeat (*Prelp*), Indian hedgehog (*Ihh*) and *Col10a1*. (**B**) Fractional length is expressed as a ratio of the measurement of a particular zone over the length of the entire growth plate (articular surface to mineralized region). *Fgfr1* expression is similar between wild-type and mutant limbs (P=0.033), but *Prelp* and *Ihh* are significantly decreased (P<0.001, P<0.005). *Col10a1* is not significantly reduced (P=0.173). Although *Fgfr1* expression is similar, the region between the epiphysis and the distal end of *Prelp* expression is significantly increased (red bracket, P<0.0001).

Piga mutant chondrocytes fail to intercalate

One intriguing observation is that although mutant chondrocytes ultimately progress through all stages of maturation, columns of discoid cells never form, suggesting that cell morphology and maturation are regulated by distinct mechanisms. Column formation in chondrocytes occurs in two steps with cell division
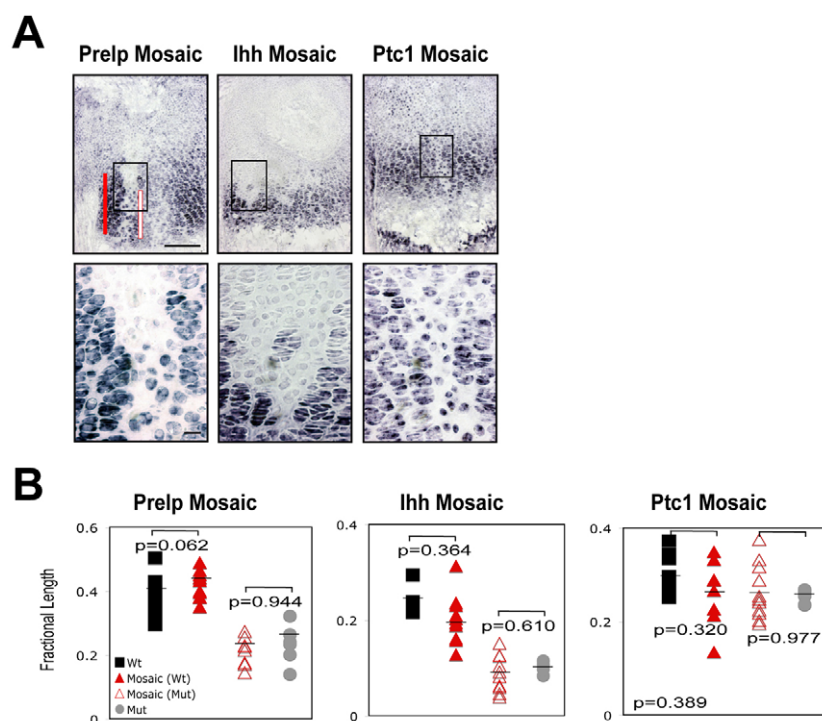
Fig. 5. Cell autonomous delay in *Piga* chondrocyte maturation. (**A**) Mutant proliferative chondrocytes express *Prelp* later in maturation than do wild-type chondrocytes in mosaic sections. This is also the case for *Ihh*. (**B**) Measurement of fractional length in wild type, mosaic and mutant growth plates. *Piga* mutant chondrocytes are not deficient in receiving all signals because the downstream target of hedgehog signaling (*Ptc1*) is expressed similarly in mutant and wild-type chondrocytes in mosaic sections (*P*=0.389). Scale bars: 200 µm for 10× images; 50 µm for 40× insets.

displacing daughters laterally before intercalation integrates them back into the column (Dodds, 1930; Li and Dudley, 2009). Absence of columns could result from defects at either step. We first determined the orientation of cell division (Fig. 6A) and showed that wild-type and mutant resting chondrocytes divide in arbitrary planes (Fig. 6B), whereas 74% of mutant proliferative chondrocytes divide at angles nearly perpendicular to the axis of growth similar to wild-type chondrocytes (Fig. 6B). Although 26% of the mutant proliferative chondrocytes divide at non-wild-type angles, these improperly aligned cell divisions cannot account for the 100% of mutant chondrocytes that fail to form columns, which suggests that the primary defect is not in establishing the division plane.

Next, we tested for defects in cell intercalation. Initially, we considered using the *lacZ* cassette embedded in the conditional *Piga* allele to label mutant cells, but we found that the *lacZ* gene product was not detectable using chromogenic substrates, immunofluorescence or ISH. Therefore, we used a property of *TOPGAL* transgene expression – patchy across the tissue but uniform within a chondrocyte column – to test whether *Piga* null cells intercalate into columns. Because cells within an individual column derive from a single progenitor cell, epigenetic regulation of *TOPGAL* results in a short-term lineage mark (Fig. 6C). We analyzed groups of labeled cells in TOPGAL mice that were additionally wild-type or mutant for *Piga* (Fig. 6C). Because chondrocytes in wild-type columns undergo limited cell divisions (Dodds, 1930), we determined total cell number and extent of lateral dispersion in small groups of labeled cells (<16 cells/group). Labeled wild-type cells are contained in groups distributed in the longitudinal axis that are generally one or two cell diameters wide (Fig. 6C,D). By contrast, mutant cells were preferentially distributed laterally within the growth plate (*P*<0.0001, compared with wild type; Fig. 6D). Consistent with this, we found that groups of *Piga* mutant cells were smaller than wild type (*P*<0.0001), presumably a result of the lateral spread of progeny into adjacent sections.

Failure of column formation could also result from defects in cytokinesis, as shown for integrin β1 mutant chondrocytes (Aszodi et al., 2003). However, in *Piga* mutants, chondrocytes showed normal cell surface display of integrin β1, and multinucleate or apoptotic cells normally associated with cytokinesis defects were not observed (Fig. 3B; see also Fig. S7 in the supplementary material; data not shown). Moreover, we found in both wild-type and mutant cartilage that dividing cells in the resting and proliferative zones showed a normal flattened interface that included a well-formed midbody (Fig. 6E), a microtubule-based structure assembled during anaphase that is important for completion of cytokinesis (Raich et al., 1998). These observations suggest that cell division occurs normally in *Piga* mutants and thus the requirement for gpi-anchored proteins is in the downstream cell intercalation process.

Gpi-anchored proteins regulate cell polarity

The requirement for gpi-anchored proteins for polarized cell movements in cartilage and in axis formation in the axolotol and zebrafish suggests that gpi-anchored proteins are general components of polarity pathways (Drawbridge and Steinberg, 2000; Topczewski et al., 2001; Shao et al., 2009). We tested this hypothesis using the sensory epithelium of the vertebrate inner ear. The sensory epithelium contains four rows of hair cells each displaying a 'V'-shaped bundle of actin-rich stereocilia with a single microtubule-based kinocilium at the apex (reviewed by Kelly and Chen, 2007). Alignment of stereocilia and kinocilium across all hair cells in wild-type cochlea is regulated by the PCP pathway (reviewed by Klein and Mlodzik, 2005). To test whether gpi-anchored proteins regulate cell polarity, we crossed X^{Piga}/X^{Piga} females to $Foxg1^{tm1(cre)Skm}$ males, which express Cre recombinase in the otic vessel (Hebert and McConnell, 2000). Hair cells in *Piga* mutant ears display disrupted architecture at the base of the hair cells and poorly aligned stereocilia and kinocilia of the outer hair cell layers (Fig. 7A-C), as has been shown for PCP mutants such as *Vangl2* and scribble (Montcouquiol et al., 2003). Additionally, Vangl2 is mislocalized in *Piga* mutant
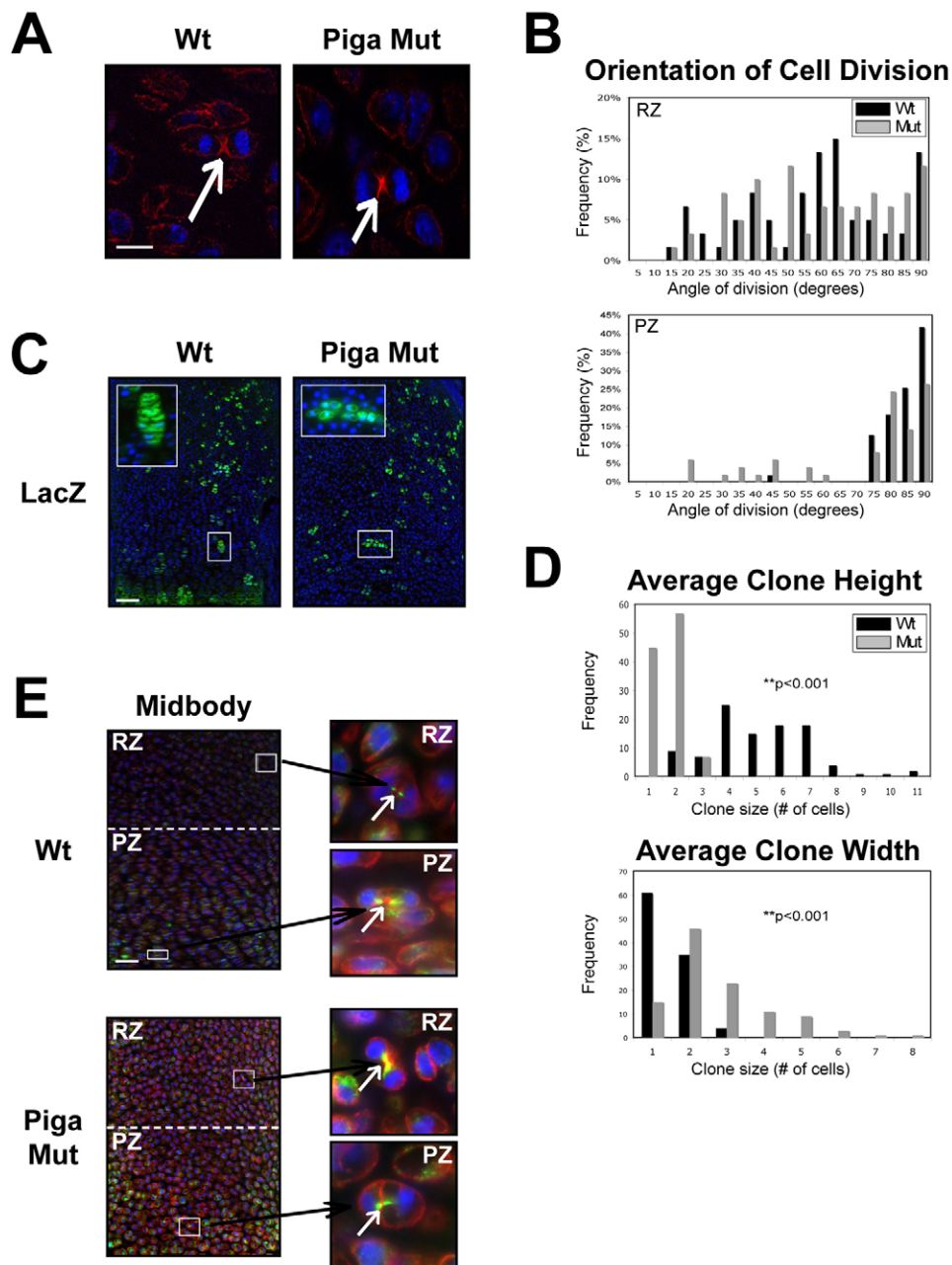
Fig. 6. *Piga* mutant chondrocytes fail to intercalate into columns. (**A**) Daughter cells were identified by phalloidin labeling (red) of the cleavage furrow (white arrow); nuclei are stained with DAPI. (**B**) RZ chondrocytes divide at arbitrary angles, whereas the PZ chondrocytes for both wild-type and mutant growth plates divide nearly perpendicular to the long axis of the bone ($\theta \sim 90°$; distinct from resting cells $P < 0.0001$). (**C**) Canonical Wnt signaling is unaltered in *Piga* mutant chondrocytes, as measured by β-galactosidase (β-gal) activity from the *TOPGAL* reporter. The patchy β-gal staining corresponds to clonally related chondrocytes. (**D**) In the proliferative zone, the total number of cells in a clone and the clone width were counted, revealing that *Piga* mutant clones are significantly wider ($P < 0.0001$) and shorter ($P < 0.0001$) than wild-type clones. (**E**) The midbody (acetylated tubulin, green) connects the dividing daughter cells in both wild-type and mutant chondrocytes. Scale bars: in A, 50 μm; in C, 200 μm; in E, 100 μm.

outer hair cells (Fig. 7C). Collectively, our data establish a link between gpi-anchored protein activity and tissue polarity pathways that pattern the sensory epithelium of the inner ear.

DISCUSSION
Gpi-anchored proteins function cell autonomously
Conditional inactivation of *Piga* results in the loss of gpi-anchored cell surface proteins, as determined by the absence of Alp activity on mutant chondrocytes and osteoblasts, the lack of Gpc3 on mutant chondrocytes, and the failure of transfected mutant chondrocytes to display gpi-anchored Gfp, findings that are consistent with previous studies in the hematopoietic lineage (Tremml et al., 1999). Interestingly, Alp activity is not observed in the matrix of mutant cartilage, demonstrating that secreted forms are not generated by the absence of anchor addition. This finding is consistent with previous studies demonstrating that

failure of anchor addition leads to retention in the endoplasmic reticulum (Field et al., 1994; Doering and Schekman, 1996; Doering and Schekman, 1997) and protein degradation (Ali et al., 2000). In this context, the presence of secreted epitope-tagged gpi-anchored Knypek in zebrafish embryos injected with morpholinos directed against *pigp* (Shao et al., 2009) suggests an incomplete knockdown of transamidase activity. However, secreted forms, if they exist, probably do not act dominantly because small patches of wild-type or mutant cells surrounded by cells of the opposite genotype are readily observed in mosaic females. Moreover, in mosaics, transitions in maturation state for cells of one genotype are unaffected by the presence of large numbers of cells of the opposite genotype. Together, these data indicate that the observed phenotype is the result of cell autonomous *Piga* expression and does not reflect global defects in signaling pathways that regulate growth plate function.
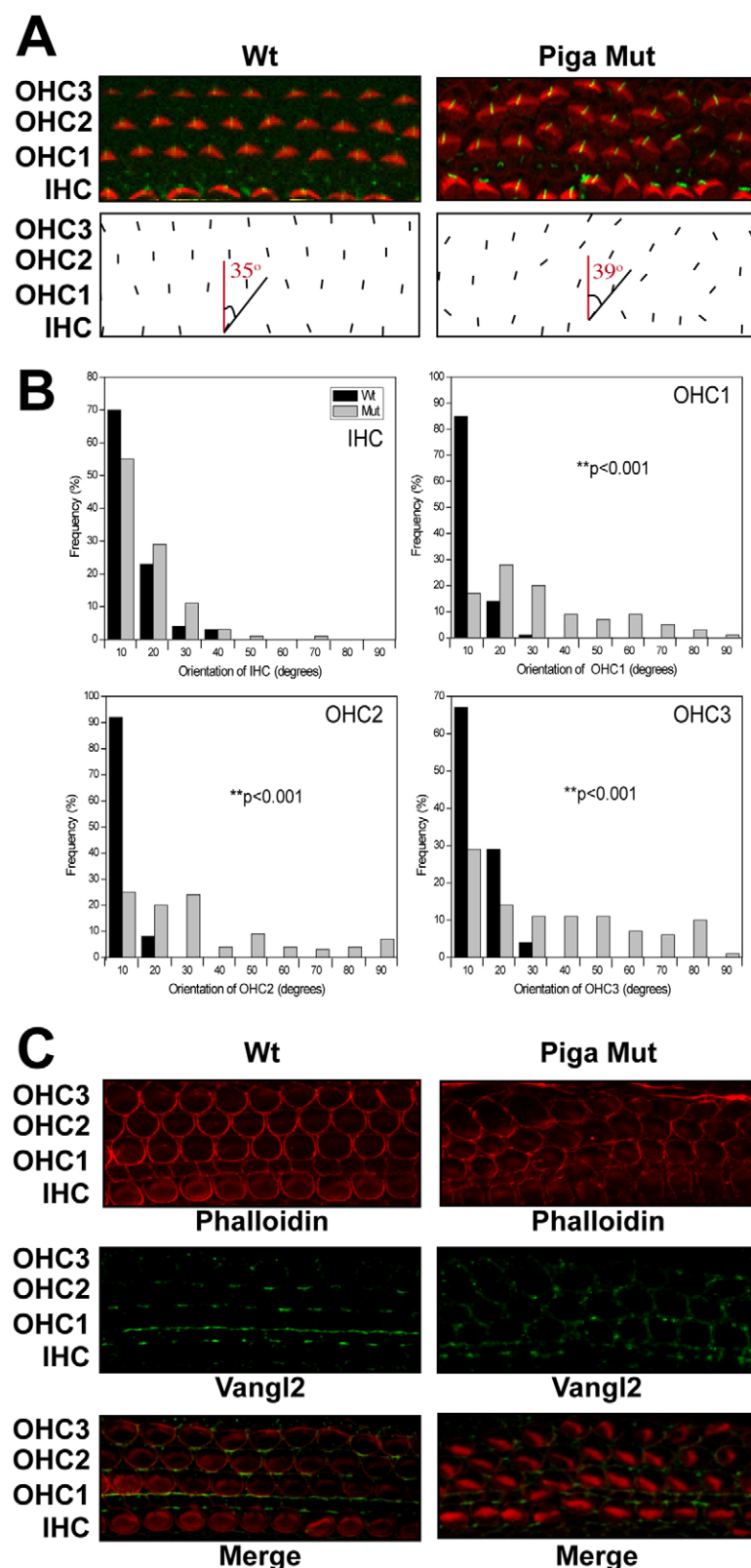
Fig. 7. Gpi-anchored proteins regulate polarity in hair cells. (**A**) Stereocilia labeled with phalloidin (red) and kinocilia labeled with acetylated tubulin (green) are organized with the apex at an ~90° angle to the basal surface of the cochlea. Hair cell orientation was calculated by measuring the angle that the kinocilia deviate from 90°. (**B**) *Piga* mutant inner hair cells have normal orientation (*P*=0.092). *Piga* mutant outer hair cells are significantly perturbed (OHC1, *P*=0; OHC2, *P*=0; OHC3, *P*<0.0001). (**C**) Phalloidin (red) and Vangl2 (green) show that *Piga* mutant outer hair cells have aberrant architecture and reduced localization of Vangl2 compared with wild type.

Gpi-anchored proteins are not required for tissue patterning

Numerous studies have demonstrated important roles for gpi-anchored cell surface proteins in controlling cell signaling and cell adhesion during embryogenesis. For example, *dally* and *dally-like* encode two gpi-anchored HSPGs of the glypican family that contribute to patterning of the *Drosophila* wing through the regulation of signaling by secreted factors of the Wg/Wnt and Hh families (Lin and Perrimon, 1999; Tsuda et al., 1999; Lum et al., 2003; Kirkpatrick et al., 2004). In the vertebrate limb, gpi-anchored

ephrin A ligands are proposed to regulate cell sorting in the autopod through interaction with the EphA4 and/or EphA7 receptor tyrosine kinase (Wada et al., 1998; Stadler et al., 2001), and a gradient of CD59 has been linked to regeneration of the proximodistal axis in amputated newt limbs (da Silva et al., 2002; Kumar et al., 2007). By contrast, elimination of *Piga* expression in the posterior LPM lineage does not alter patterning of the limb skeleton. Even mosaic limbs do not show patterning defects predicted from errors in cell sorting (Davy et al., 2004). One caveat to this interpretation is that we do not currently have robust assays to verify the absence of gpi-anchored proteins in the early embryonic limb buds. However, given that *Hoxb6::cre* catalyzes near complete recombination in the LPM by 9.5 dpc (Lowe et al., 2000), it is reasonable to assume that mutant early limb mesenchyme cannot generate new gpi-anchored proteins. Proteins produced before 9.5 dpc could function early but would be rapidly diluted as local cell proliferation drives limb bud growth. Thus, total depletion of gpi-anchored proteins is likely to occur early in limb bud development and certainly before digit formation when the gpi-anchored ephrin A ligands are supposed to act (Wada et al., 1998; Stadler et al., 2001).

The nonessential function of gpi-anchored proteins is not limited to the cartilage, as we show that loss of *Piga* expression in the otic placode does not alter the gross structure of the inner ear, although hair cells in the cochlea do display altered cell polarity. Similarly, defective gpi-anchoring of proteins does not substantially affect patterning of the skin (Hara-Chikuma et al., 2004), the neural tube (Nozaki et al., 1999), or the zebrafish embryonic germ layers (Shao et al., 2009). Despite potential effects on key growth factor signaling pathways, gpi-anchored proteins are not absolutely required for many processes. This might reflect compensation by, or predominance of, a non-gpi-anchored protein. For example, mosaics for a null mutation in the non-gpi-anchored ephrin B1 ligand show defects in cell sorting and patterning predicted for loss of ephrin A ligands in the vertebrate limb (Davy et al., 2004). Thus, the gpi-anchored class of cell surface proteins might primarily function to fine-tune cell-cell interaction pathways to promote robustness.

Gpi-anchored proteins regulate chondrocyte maturation

Loss of gpi-anchored proteins leads to a reduced rate of chondrocyte maturation that is first observed at the transition from resting to proliferative chondrocytes, as demonstrated by the decreased size of the proliferative zone despite an increase in resting chondrocyte proliferation. The size of and transitions between maturation zones are controlled by the action of a complex network of synergistic and antagonistic pathways regulated by secreted signaling proteins (Karsenty and Wagner, 2002; Kronenberg, 2003; Yang et al., 2003). HSPGs, including gpi-anchored glypicans, are important regulators of these signaling pathways (reviewed by Häcker et al., 2005). In cartilage, HSPGs might determine the extracellular distribution of secreted ligands (Koziel et al., 2004). However, in mosaics, in which wild-type cells display normal zones of maturation consistent with normal ligand distribution, *Piga* null cells show delayed onset and reduced size of maturation zones equivalent to that in mutant cartilage. The failure to initiate transitions in maturation state synchronously with wild-type neighboring cells suggests that *Piga* null cells either do not correctly detect or fail to respond appropriately to growth plate signals.

Defects in signaling are consistent with a role for gpi-anchored proteins as co-receptors for signals that promote chondrocyte maturation, or as antagonists of factors that repress maturation.

Likely candidates for these functions are gpi-anchored HSPGs of the glypican family. Consistent with this interpretation, many similarities exist between mutants in *Ext1* (Koziel et al., 2004), an enzyme involved in the production of HSPGs, and *Piga* (see Table S1 in the supplementary material). Interestingly, a hypomorphic allele of *Gpc3* displays defects in chondrocyte maturation similar to those of *Piga* mutants, suggesting that Gpc3 is the primary gpi-anchored regulator of chondrocyte maturation in the growth plate (Viviano et al., 2005). If so, it will be important to determine the functions of the other glypicans expressed in the growth plate (see Fig. S3 in the supplementary material).

Gpi-anchored proteins regulate tissue polarity

The fact that *Piga* null cells eventually pass through all phases of chondrocyte maturation while defects in cell shape and cell arrangement in proliferative chondrocytes are absolute suggests that distinct mechanisms regulate chondrocyte maturation and proliferative chondrocyte behavior. The arrangement of proliferative chondrocytes into columns of stacked cells is a multi-step process that includes two planar processes – aligned division planes and cell intercalation – and that is regulated by non-canonical Fzd signaling (Dodds, 1930; Li and Dudley, 2009).

In the absence of gpi-anchored proteins, the spindle orienting mechanism is functional, but imprecise, resulting in a percentage of chondrocytes that divide out of plane. A similar percentage of misaligned division planes are observed in kidney tubules lacking the atypical cadherin Fat4, a component of the PCP pathway (Saburi et al., 2008). However, the *Fat4* mutant phenotype is more severe than that of *Piga* mutants in that a substantial number of *Fat4* mutant cells align the mitotic spindle orthogonal to wild type. In this respect, the *Fat4* phenotype approximates, but is less severe than, the uniform distribution of division planes in chick chondrocytes deficient in non-canonical Fzd signaling (Li and Dudley, 2009). Although gpi-anchored glypicans are components of the non-canonical Fzd pathway (Caneparo et al., 2007; Shao et al., 2009), the weak division plane phenotype of *Piga* mutants suggests that gpi-anchored proteins either are largely expendable because of redundancy or are not core components of the Fzd pathway that regulates the division plane. In this latter model, one possibility is that gpi-anchored proteins regulate a parallel process that influences the division plane. For example, division of most cells occurs according to Hertwig's rule, which predicts alignment of the mitotic spindles parallel to the long axis of the cell (Wilson, 1900; Wilson, 1925), and might involve interaction between cell-matrix adhesion and the actin cytoskeleton (Toyoshima and Nishida, 2007). Even though tissue polarity pathway function can override Hertwig's rule (Gong et al., 2004), perhaps the system is more robust when components of polarity pathways are aligned with a prominent axis defined by cell shape/cell adhesion that might be lacking in round *Piga* chondrocytes.

Interestingly, although the plane of cell division is largely normal, mutant cells fail to intercalate and, as a result, clones of *Piga* null cells expand laterally across the proliferative zone instead of forming columns aligned to the longitudinal axis. It remains to be determined if the small number of stacked chondrocytes in a mutant clone results from occasional, normal cell intercalation events or from aberrant division planes in a non-intercalating clone. Nonetheless, these results refine our previous model (Li and Dudley, 2009) by demonstrating that establishment of the division plane and the process of cell intercalation are differentially regulated, despite both events being sensitive to non-canonical Fzd signaling. Moreover, lateral expansion of the proliferative chondrocytes

correlates with the increased width and decreased longitudinal growth of mutant cartilage, providing further evidence that cell intercalation events orient both local and tissue-wide vectors of growth in cartilage through a process of CE.

Towards a mechanism of convergent extension in cartilage

How cell polarity pathways influence cell shape and promote cell intercalation is currently under debate. One possibility is that gpi-anchored proteins regulate non-canonical Fzd signaling. In this regard, two non-exclusive models have been proposed for the role of the gpi-anchored proteins in CE. First, the glypican Knypek has been shown to act in conjunction with the secreted canonical pathway inhibitor Dickkopf (Dkk) to alter the specificity of Fzd signaling from activating canonical to activating non-canonical pathways (Caneparo et al., 2007). Second, gpi-anchored proteins might stabilize Fzd receptors on the cell surface potentially promoting membrane localization of Dishevelled, an event associated with non-canonical PCP signaling (Shao et al., 2009). In this context, the observation of reduced Vangl2 localization in hair cells might reflect defects in Fzd signaling rather than a direct interaction between Vangl2 and gpi-anchored proteins.

The effectors of cell polarity pathways are most probably regulators of cytoskeletal dynamics and cell-matrix interactions. In particular, matrix structure is an important determinant of cell shape and cell intercalation (Davidson et al., 2006). Consistent with this, null mutants in cartilage-specific *Col9a1* (Blumbach et al., 2008; Dreier et al., 2008) and the cell-matrix adhesion receptor integrin β1 (Aszodi et al., 2003) result in round, disorganized proliferative chondrocytes that are grossly similar to those of *Piga* mutants. However, loss of either integrin β1 or *Col9a1* function results in a more severe phenotype than displayed by *Piga* null cartilage, and expression of *Col9a1* and cell surface localization of integrin β1 are unaffected in *Piga* mutant cartilage (see Figs S4, S6 in the supplementary material). Together, these data suggest that gpi-anchored proteins do not regulate the production of *Col9a1* or integrin β1. Thus, as with Fzd receptors, gpi-anchored proteins might be required for the appropriate trafficking or stability of cell adhesion molecules, or to properly organize the extracellular matrix to promote column formation.

Conclusions

CE and PCP are two processes that define the cellular architecture of many tissues. Although once thought to be highly specific to certain tissues, these processes are being discovered in diverse cell types, including chondrocytes. The involvement of non-canonical Fzd signaling, Rho GTPase activity, and now gpi-anchored proteins in both CE and PCP suggests that common mechanisms regulate the architecture of all tissues.

Supplementary material

Supplementary material for this article is available at
http://dev.biologists.org/cgi/content/full/136/20/3463/DC1

References

Abad, V., Meyers, J. L., Weise, M., Gafni, R. I., Barnes, K. M., Nilsson, O., Bacher, J. D. and Baron, J. (2002). The role of the resting zone in growth plate chondrogenesis. *Endocrinology* **143**, 1851-1857.

Ali, B. R., Claxton, S. and Field, M. C. (2000). Export of a misprocessed gpi-anchored protein from the endoplasmic reticulum in vitro in an ATP- and cytosol-dependent manner. *FEBS Lett.* **483**, 32-36.

Arikawa-Hirasawa, E., Watanabe, H., Takami, H., Hassell, J. R. and Yamada, Y. (1999). Perlecan is essential for cartilage and cephalic development. *Nat. Genet.* **23**, 354-358.

Aszodi, A., Hunziker, E. B., Brakebusch, C. and Fassler, R. (2003). Beta1 integrins regulate chondrocyte rotation, G1 progression, and cytokinesis. *Genes Dev.* **17**, 2465-2479.

Bernfield, M., Gotte, M., Park, P. W., Reizes, O., Fitzgerald, M. L., Lincecum, J. and Zako, M. (1999). Functions of cell surface heparan sulfate proteoglycans. *Annu. Rev. Biochem.* **68**, 729-777.

Blumbach, K., Niehoff, A., Paulsson, M. and Zaucke, F. (2008). Ablation of collagen IX and COMP disrupts epiphyseal cartilage architecture. *Matrix Biol.* **27**, 306-318.

Brault, V., Moore, R., Kutsch, S., Ishibashi, M., Rowitch, D. H., McMahon, A. P., Sommer, L., Boussadia, O. and Kemler, R. (2001). Inactivation of the beta-catenin gene by Wnt1-Cre-mediated deletion results in dramatic brain malformation and failure of craniofacial development. *Development* **128**, 1253-1264.

Caneparo, L., Huang, Y. L., Staudt, N., Tada, M., Ahrendt, R., Kazanskaya, O., Niehrs, C. and Houart, C. (2007). Dickkopf-1 regulates gastrulation movements by coordinated modulation of Wnt/beta catenin and Wnt/PCP activities, through interaction with the Dally-like homolog Knypek. *Genes Dev.* **21**, 465-480.

da Silva, S. M., Gates, P. B. and Brockes, J. P. (2002). The newt ortholog of CD59 is implicated in proximodistal identity during amphibian limb regeneration. *Dev. Cell* **3**, 547-555.

DasGupta, R. and Fuchs, E. (1999). Multiple roles for activated LEF/TCF transcription complexes during hair follicle development and differentiation. *Development* **126**, 4557-4568.

Davidson, L. A., Marsden, M., Keller, R. and Desimone, D. W. (2006). Integrin alpha5beta1 and fibronectin regulate polarized cell protrusions required for Xenopus convergence and extension. *Curr. Biol.* **16**, 833-844.

Davy, A., Aubin, J. and Soriano, P. (2004). Ephrin-B1 forward and reverse signaling are required during mouse development. *Genes Dev.* **18**, 572-583.

Dodds, G. (1930). Row formation and other types of arrangement of cartilage cells in endochondral ossification. *Anat. Rec.* **46**, 385-399.

Doering, T. L. and Schekman, R. (1996). Gpi anchor attachment is required for Gas1p transport from the endoplasmic reticulum in COPII vesicles. *EMBO J.* **15**, 182-191.

Doering, T. L. and Schekman, R. (1997). Glycosylphosphatidylinositol anchor attachment in a yeast in vitro system. *Biochem. J.* **328**, 669-675.

Drawbridge, J. and Steinberg, M. S. (2000). Elongation of axolotl tailbud embryos requires gpi-linked proteins and organizer-induced active ventral trunk endoderm cell rearrangements. *Dev. Biol.* **223**, 27-37.

Dreier, R., Opolka, A., Grifka, J., Bruckner, P. and Grassel, S. (2008). Collagen IX-deficiency seriously compromises growth cartilage development in mice. *Matrix Biol.* **27**, 319-329.

Field, M. C., Moran, P., Li, W., Keller, G. A. and Caras, I. W. (1994). Retention and degradation of proteins containing an uncleaved glycosylphosphatidylinositol signal. *J. Biol. Chem.* **269**, 10830-10837.

Gong, Y., Mo, C. and Fraser, S. E. (2004). Planar cell polarity signalling controls cell division orientation during zebrafish gastrulation. *Nature* **430**, 689-693.

Häcker, U., Nybakken, K. and Perrimon, N. (2005). Heparan sulphate proteoglycans: the sweet side of development. *Nat. Rev. Mol. Cell Biol.* **6**, 530-541.

Hara-Chikuma, M., Takeda, J., Tarutani, M., Uchida, Y., Holleran, W. M., Endo, Y., Elias, P. M. and Inoue, S. (2004). Epidermal-specific defect of gpi anchor in Pig-a null mice results in Harlequin Ichthyosis-like features. *J. Invest. Dermatol.* **123**, 464-469.

Hebert, J. M. and McConnell, S. K. (2000). Targeting of cre to the Foxg1 (BF-1) locus mediates loxP recombination in the telencephalon and other developing head structures. *Dev. Biol.* **222**, 296-306.

Horiki, M., Imamura, T., Okamoto, M., Hayashi, M., Murai, J., Myoui, A., Ochi, T., Miyazono, K., Yoshikawa, H. and Tsumaki, N. (2004). Smad6/Smurf1 overexpression in cartilage delays chondrocyte hypertrophy and causes dwarfism with osteopenia. *J. Cell. Biol.* **165**, 433-445.

Howlett, C. R. (1979). The fine structure of the proximal growth plate of the avian tibia. *J. Anat.* **128**, 377-399.

Howlett, C. R. (1980). The fine structure of the proximal growth plate and metaphysis of the avian tibia: endochondral osteogenesis. *J. Anat.* **130**, 745-768.

Hunziker, E. B., Kapfinger, E. and Saager, C. (1999). Hypertrophy of growth plate chondrocytes in vivo is accompanied by modulations in the activity state

and surface area of their cytoplasmic organelles. *Histochem. Cell Biol.* **112**, 115-123.

Ide, H., Wada, N. and Uchiyama, K. (1994). Sorting out of cells from different parts and stages of the chick limb bud. *Dev. Biol.* **162**, 71-76.

Karp, S. J., Schipani, E., St-Jacques, B., Hunzelman, J., Kronenberg, H. and McMahon, A. P. (2000). Indian hedgehog coordinates endochondral bone growth and morphogenesis via parathyroid hormone related-protein-dependent and -independent pathways. *Development* **127**, 543-548.

Karsenty, G. and Wagner, E. F. (2002). Reaching a genetic and molecular understanding of skeletal development. *Dev. Cell* **2**, 389-406.

Kawagoe, K., Takeda, J., Endo, Y. and Kinoshita, T. (1994). Molecular cloning of murine pig-a, a gene for GPI-anchor biosynthesis, and demonstration of interspecies conservation of its structure, function, and genetic locus. *Genomics* **23**, 566-574.

Kawaguchi, J., Wilson, V. and Mee, P. J. (2002). Visualization of whole-mount skeletal expression patterns of LacZ reporters using a tissue clearing protocol. *Biotechniques* **32**, 66-70.

Keller, P., Tremml, G., Rosti, V. and Bessler, M. (1999). X inactivation and somatic cell selection rescue female mice carrying a Piga-null mutation. *Proc. Natl. Acad. Sci. USA* **96**, 7479-7483.

Keller, P., Payne, J. L., Tremml, G., Greer, P. A., Gaboli, M., Pandolfi, P. P. and Bessler, M. (2001). FES-Cre targets phosphatidylinositol glycan class A (PIGA) inactivation to hematopoietic stem cells in the bone marrow. *J. Exp. Med.* **194**, 581-589.

Kelly, M. and Chen, P. (2007). Shaping the mammalian auditory sensory organ by the planar cell polarity pathway. *Int. J. Dev. Biol.* **51**, 535-547.

Kirkpatrick, C. A., Dimitroff, B. D., Rawson, J. M. and Selleck, S. B. (2004). Spatial regulation of Wingless morphogen distribution and signaling by Dally-like protein. *Dev. Cell* **7**, 513-523.

Klein, T. J. and Mlodzik, M. (2005). Planar cell polarization: an emerging model points in the right direction. *Annu. Rev. Cell Dev. Biol.* **21**, 155-176.

Kostova, Z., Rancour, D. M., Menon, A. K. and Orlean, P. (2000). Photoaffinity labelling with P2-(4-azidoanilido)uridine 5′triphosphate identifies gpi3p as the USP-GlcNAc-binding subunit of the enzyme that catalyses formation of GlcNAc-phosphatidylinositol, the first glycolipid intermediate in glycosylphosphatidylinositol synthesis. *Biochem. J.* **350**, 815-822.

Koziel, L., Kunath, M., Kelly, O. G. and Vortkamp, A. (2004). Ext1-dependent heparan sulfate regulates the range of Ihh signaling during endochondral ossification. *Dev. Cell* **6**, 801-813.

Kratochwil, K., Ghaffari-Tabrizi, N., Holzinger, I. and Harbers, K. (1993). Restricted expression of Mov13 mutant alpha 1(I) collagen gene in osteoblasts and its consequences for bone development. *Dev. Dyn.* **198**, 273-283.

Kronenberg, H. M. (2003). Developmental regulation of the growth plate. *Nature* **423**, 332-336.

Kumar, A., Gates, P. B. and Brockes, J. P. (2007). Positional identity of adult stem cells in salamander limb regeneration. *C. R. Biol.* **330**, 485-490.

Li, Y. and Dudley, A. T. (2009). Noncanonical Frizzled signaling regulates cell polarity in growth plate chondrocytes. *Development* **136**, 1083-1092.

Lin, X. and Perrimon, N. (1999). Dally cooperates with Drosophila Frizzled 2 to transduce Wingless signalling. *Nature* **400**, 281-284.

Logan, M., Martin, J. F., Nagy, A., Lobe, C., Olson, E. N. and Tabin, C. J. (2002). Expression of Cre Recombinase in the developing mouse limb bud driven by a Prxl enhancer. *Genesis* **33**, 77-80.

Lowe, L. A., Yamada, S. and Kuehn, M. R. (2000). HoxB6-Cre transgenic mice express Cre recombinase in extra-embryonic mesoderm, in lateral plate and limb mesoderm and at the midbrain/hindbrain junction. *Genesis* **26**, 118-120.

Lum, L., Yao, S., Mozer, B., Rovescalli, A., Von Kessler, D., Nirenberg, M. and Beachy, P. A. (2003). Identification of Hedgehog pathway components by RNAi in Drosophila cultured cells. *Science* **299**, 2039-2045.

Magnusson, P., Larsson, L., Magnusson, M., Davie, M. W. and Sharp, C. A. (1999). Isoforms of bone alkaline phosphatase: characterization and origin in human trabecular and cortical bone. *J. Bone Miner. Res.* **14**, 1926-1933.

McLeod, M. J. (1980). Differential staining of cartilage and bone in whole mouse fetuses by alcian blue and alizarin red S. *Teratology* **22**, 299-301.

Miyata, T., Takeda, J., Iida, Y., Yamada, N., Inoue, N., Takahashi, M., Maeda, K., Kitani, T. and Kinoshita, T. (1993). The cloning of PIG-A, a component in the early step of GPI-anchor biosynthesis. *Science* **259**, 1318-1320.

Montcouquiol, M., Rachel, R. A., Lanford, P. J., Copeland, N. G., Jenkins, N. A. and Kelley, M. W. (2003). Identification of Vangl2 and Scrb1 as planar polarity genes in mammals. *Nature* **423**, 173-177.

Murtaugh, L. C., Chyung, J. H. and Lassar, A. B. (1999). Sonic hedgehog promotes somitic chondrogenesis by altering the cellular response to BMP signaling. *Genes Dev.* **13**, 225-237.

Nicholson, D. W., Ali, A., Thornberry, N. A., Vaillancourt, J. P., Ding, C. K., Gallant, M., Gareau, Y., Griffin, P. R., Labelle, M., Lazebnik, Y. A. et al. (1995). Identification and inhibition of the ICE/CED-3 protease necessary for mammalian apoptosis. *Nature* **376**, 37-43.

Noonan, K. J., Hunziker, E. B., Nessler, J. and Buckwalter, J. A. (1998). Changes in cell, matrix compartment, and fibrillar collagen volumes between growth-plate zones. *J. Orthop. Res.* **16**, 500-508.

Nozaki, M., Ohishi, K., Yamada, N., Kinoshita, T., Nagy, A. and Takeda, J. (1999). Developmental abnormalities of glycosylphosphatidylinositol-anchor-deficient embryos revealed by cre/loxP system. *Lab. Invest.* **79**, 293-299.

Paulick, M. G. and Bertozzi, C. R. (2008). The glycosylphosphatidylinositol anchor: a complex membrane-anchoring structure for proteins. *Biochemistry* **47**, 6991-7000.

Pizauro, J. M., Ciancaglini, P. and Leone, F. A. (1994). Osseous plate alkaline phosphatase is anchored by GPI. *Braz. J. Med. Biol. Res.* **27**, 453-456.

Qian, D., Jones, C., Rzadzinska, A., Mark, S., Zhang, X., Steel, K. P., Dai, X. and Chen, P. (2007). Wnt5a functions in planar cell polarity regulation in mice. *Dev. Biol.* **306**, 121-133.

Raich, W. B., Moran, A. N., Rothman, J. H. and Hardin, J. (1998). Cytokinesis and midzone microtubule organization in Caenorhabditis elegans require the kinesin-like protein ZEN-4. *Mol. Cell. Biol.* **9**, 2037-2049.

Rosti, V., Tremml, G., Soares, V., Pandolfi, P. P., Luzzatto, L. and Bessler, M. (1997). Murine embryonic stem cells without pig-a gene activity are competent for hematopoiesis with the PNH phenotype but not for clonal expansion. *J. Clin. Invest.* **100**, 1028-1036.

Saburi, S., Hester, I., Fischer, E., Pontoglio, M., Eremina, V., Gessler, M., Quaggin, S. E., Harrison, R., Mount, R. and McNeill, H. (2008). Loss of Fat4 disrupts PCP signaling and oriented cell division and leads to cystic kidney disease. *Nat. Genetics* **40**, 1010-1015.

Shao, M., Liu, Z. Z., Wang, C. D., Li, H. Y., Carron, C., Zhan, H. W. and Shi, D. L. (2009). Down syndrome critical region protein 5 regulates membrane localization of Wnt receptors, Dishevelled stability and convergent extension in vertebrate embryos. *Development* **136**, 2121-2131.

Sommer, B., Bickel, M., Hofstetter, W. and Wetterwald, A. (1996). Expression of matrix proteins during the development of mineralized tissues. *Bone* **19**, 371-380.

St-Jacques, B., Hammerschmidt, M. and McMahon, A. P. (1999). Indian hedgehog signaling regulates proliferation and differentiation of chondrocytes and is essential for bone formation. *Genes Dev.* **13**, 2072-2086.

Stadler, H. S., Higgins, K. M. and Capecchi, M. R. (2001). Loss of Eph-receptor expression correlates with loss of cell adhesion and chondrogenic capacity in Hoxa13 mutant limbs. *Development* **128**, 4177-4188.

Topczewski, J., Sepich, D. S., Myers, D. C., Walker, C., Amores, A., Lele, Z., Hammerschmidt, M., Postlethwait, J. and Solnica-Krezel, L. (2001). The zebrafish glypican knypek controls cell polarity during gastrulation movements of convergent extension. *Dev. Cell* **1**, 251-264.

Toyoshima, F. and Nishida, E. (2007). Integrin-mediated adhesion orients the spindle parallel to the substratum in an EB1- and myosin X-dependent manner. *EMBO J.* **26**, 1487-1498.

Tremml, G., Dominguez, C., Rosti, V., Zhang, Z., Pandolfi, P. P., Keller, P. and Bessler, M. (1999). Increased sensitivity to complement and a decreased red blood cell life span in mice mosaic for a nonfunctional Piga gene. *Blood* **94**, 2945-2954.

Tsuda, M., Kamimura, K., Nakato, H., Archer, M., Staatz, W., Fox, B., Humphrey, M., Olson, S., Futch, T., Kaluza, V. et al. (1999). The cell-surface proteoglycan Dally regulates Wingless signalling in Drosophila. *Nature* **400**, 276-280.

Viviano, B. L., Silverstein, L., Pflederer, C., Paine-Saunders, S., Mills, K. and Saunders, S. (2005). Altered hematopoiesis in glypican-3-deficient mice results in decreased osteoclast differentiation and a delay in endochondral ossification. *Dev. Biol.* **282**, 152-162.

Vortkamp, A., Lee, K., Lanske, B., Segre, G. V., Kronenberg, H. M. and Tabin, C. J. (1996). Regulation of rate of cartilage differentiation by Indian hedgehog and PTH-related protein. *Science* **273**, 613-622.

Wada, N. and Ide, H. (1994). Sorting out of limb bud cells in monolayer culture. *Int. J. Dev. Biol.* **38**, 351-356.

Wada, N., Kimura, I., Tanaka, H., Ide, H. and Nohno, T. (1998). Glycosylphosphatidylinositol-anchored cell surface proteins regulate position-specific cell affinity in the limb bud. *Dev. Biol.* **202**, 244-252.

Wang, G., Woods, A., Agoston, H., Ulici, V., Glogauer, M. and Beier, F. (2007). Genetic ablation of Rac1 in cartilage results in chondrodysplasia. *Dev. Biol.* **306**, 612-623.

Watanabe, T., Inoue, N., Westfall, B., Taron, C. H., Orlean, P., Takeda, J. and Kinoshita, T. (1998). The first step of glycosylphosphatidylinositol biosynthesis is mediated by a complex of PIG-A, PIG-H, PIG-C and GPI1. *EMBO J.* **17**, 877-885.

Wilson, E. B. (1900). *The Cell in Development and Inheritance*. New York: Macmillian.

Wilson, E. B. (1925). *The Cell in Development and Heredity*, 3rd edn. New York: Macmillian.

Yamaguchi, T. P., Bradley, A., McMahon, A. P. and Jones, S. (1999). A Wnt5a pathway underlies outgrowth of multiple structures in the vertebrate embryo. *Development* **126**, 1211-1223.

Yang, Y., Topol, L., Lee, H. and Wu, J. (2003). Wnt5a and Wnt5b exhibit distinct activities in coordinating chondrocyte proliferation and differentiation. *Development* **130**, 1003-1015.
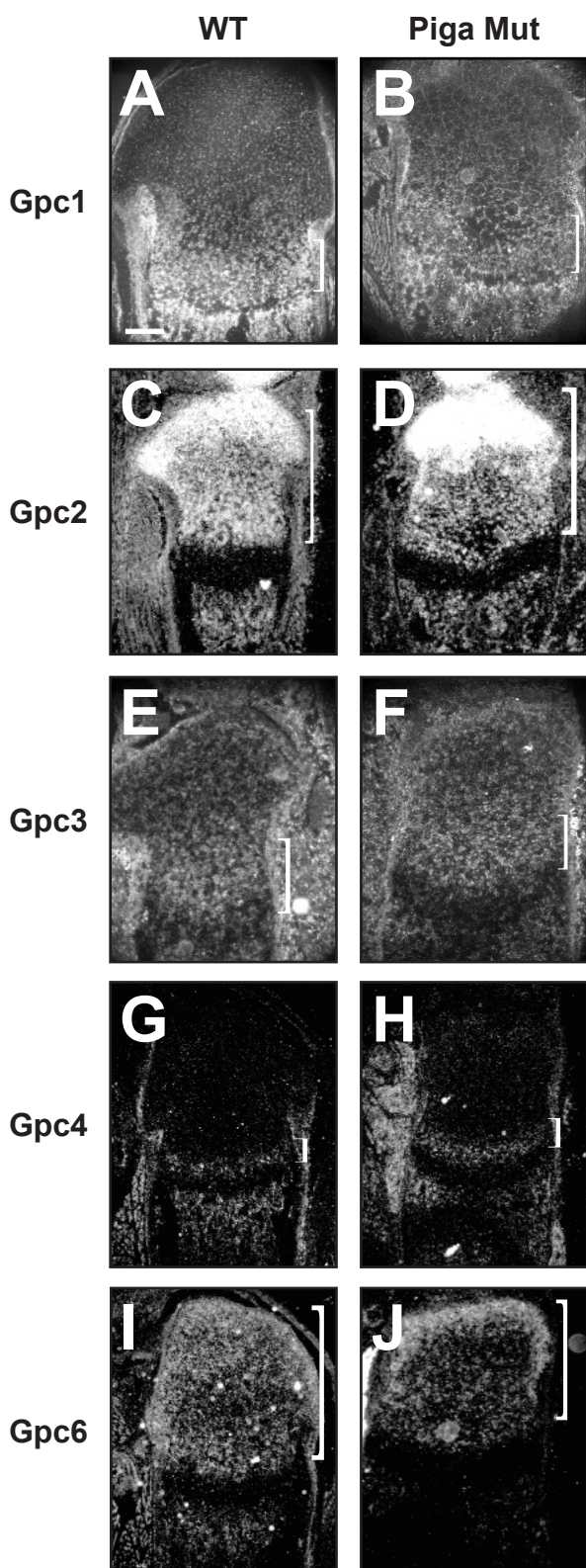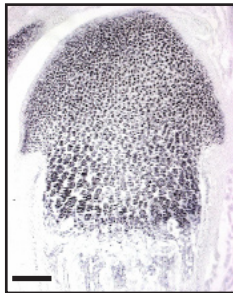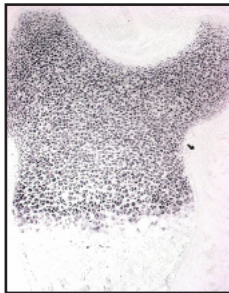
	WT	Piga Mut
VK P0		
Col 1 P0		
OC P0		
OPN P0		

WT   Piga Mut

Gpc1

Gpc2

Gpc3

Gpc4

Gpc6
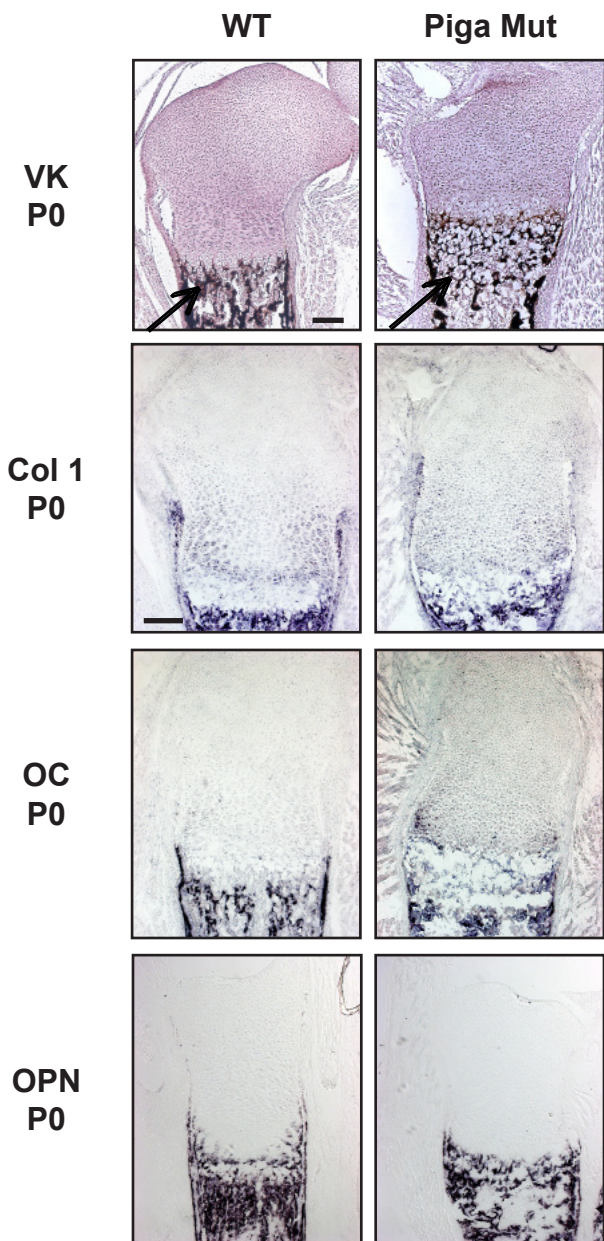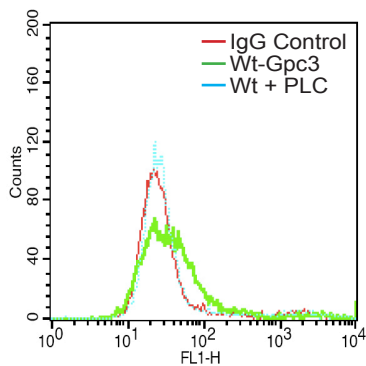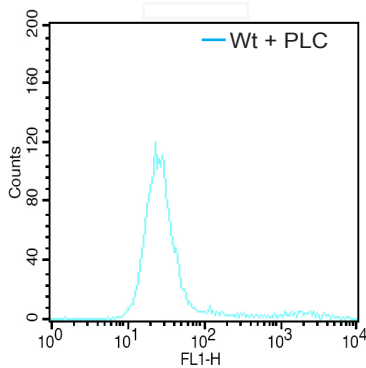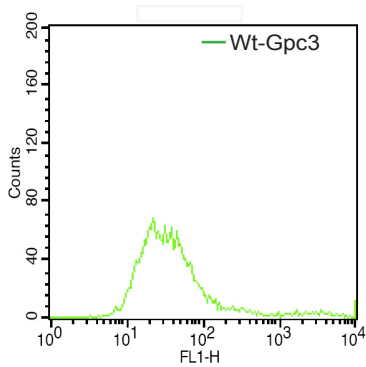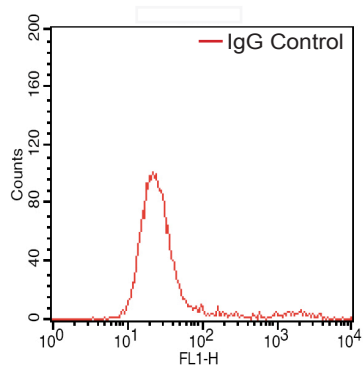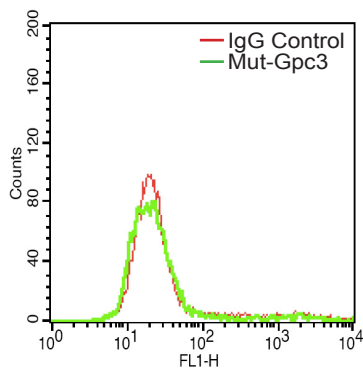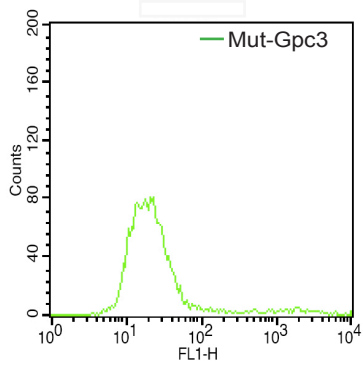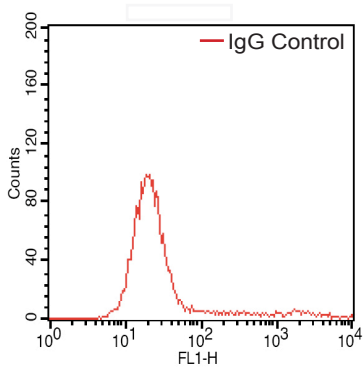
Wt **Piga Mut**

Col 9 P0

	WT	**Piga Mut**
Phospho-Smad 1/5/8		
Phospho-p44/42 MAPK		

β-Catenin Cond. KO

	Wt	Piga Mut
RZ		
PZ		
HZ		

β**1-Integrin**
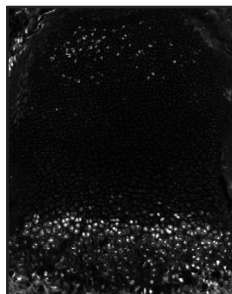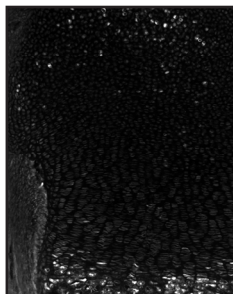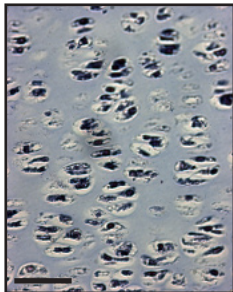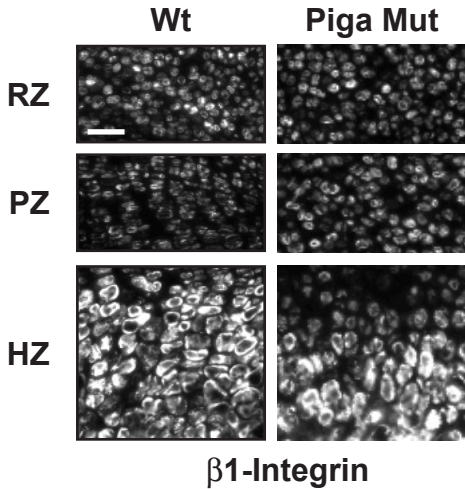
Table S1. Comparison of phenotypes of mouse mutant cartilage

Mouse line	Maturation	Bone length	Proliferation	Chondrocyte organization	References
Conditional					
$Piga \times Hoxb6$	Delay in hypertrophy	Short	RZ increased, PZ normal	Disorganized	
$Ext^{Gt/Gt}$ (hypomorph)	Delay in hypertrophy	Short	RZ increased, PZ normal	Disorganized	Koziel et al., 2004
$Ihh^{-/-}$	Delay in hypertrophy	Short	Reduced	Disorganized	St-Jacques et al., 1999
$Pthrp^{-/-}$	Increased hypertrophy	Short	Slightly reduced	Stacked properly?	Karp et al., 2000
$Ihh^{-/-}Pthrpr$*	Delay in hypertrophy	Short	Reduced	Disorganized?	Karp et al., 2000
$Ihh^{-/-}Pthrp^{-/-}$	Delay in hypertrophy	Short	?	Disorganized?	Karp et al., 2000
$Wnt5a^{-/-}$	Delay in hypertrophy	Short	RZ increased, PZ decreased	Stacked properly?	Yamaguchi et al., 1999; Yang et al., 2003
$\beta1$ integrin	Delay in ossification	Short	Reduced (binucleate cells)	Disorganized	Aszodi et al., 2003
$Rac^{fl/fl}$*	Delay in differentiation	Short	Reduced	Disorganized	Wang et al., 2007
$Col9a1^{-/-}$	?	Short	Reduced	Disorganized	Blumbach et al., 2008; Dreier et al., 2008
$Hspg2^{-/-}$ (perlecan)	?	Short	Reduced (stated, data not shown)	Disorganized	Arikawa-Hirasawa, 1999
$Smad6$*	Delay in hypertrophy	Short	Normal	Stacked properly	Horiki et al., 2004
$Gpc3^{-/-\dagger}$	Delay in hypertrophy	?	Normal	?	Viviano et al., 2005

*Activated by collagen II Cre recombinase.
†Figures show high variability in phenotype.